

# DATING AEOLIAN SEDIMENTS FROM CABO FRIO, RIO DE JANEIRO, USING TI-LI CENTER ELECTRON SPIN RESONANCE, THERMOLUMINESCENCE AND OPTICALLY STIMULATED LUMINESCENCE: A COMPARATIVE STUDY.

Lucas S. do Carmo<sup>1</sup>, Shiguo Watanabe<sup>1</sup>, Regina DeWitt<sup>2</sup>, Rafaela J. Silva<sup>3</sup>, Luiz Felipe<sup>3</sup>, José F. D. Chubaci<sup>3</sup>.

<sup>1</sup> Instituto de Pesquisas Energéticas e Nucleares (IPEN / CNEN - SP)  
Av. Professor Lineu Prestes 2242  
05508-000 São Paulo, SP  
lsatiro@usp.br

<sup>2</sup> East Carolina University (ECU)  
Luminescence Laboratory  
Howell Sciences C-209, 1000 East 5th Street  
Greenville, NC 27858, USA  
dewittr@ecu.edu

<sup>3</sup>Instituto de Física da Universidade de São Paulo (IFUSP)  
Departamento de Física Nuclear - LACIFID  
Rua do Matão, travessa R, 1371  
05508-090 São Paulo, SP  
lacifid@if.usp.br

## ABSTRACT

In this work, optically stimulated luminescence (OSL), thermoluminescence (TL) and electron spin resonance (ESR) were used to date coastal aeolian sediments from a dunefield known as Dama Branca (White Lady) in Rio de Janeiro, Brazil. Sediments have been collected from seven different points to study sand transportation and stabilization. Results obtained by those different techniques were compared. The equivalent dose ( $D_e$ ) measured by OSL, was obtained using the Single Aliquot Regenerative protocol (SAR), TL results have been corrected measuring residual TL and ESR measurements were carried out using Ti-Li center. The thermal stability of Ti-Li center was evaluated, samples were preheated to exclude the Ti-Li center thermally sensitive component. The gamma-ray spectroscopy was used to measure Uranium, Thorium and Potassium concentrations in the soil, the values were analyzed with the Dose Rate and Age Calculator (DRAC) to generate the Annual Dose Rate ( $D_r$ ). A morphological analysis showed that the dunefield has been moving influenced by semi-arid conditions and upwelling close to the coast. Ages from 0.05 to 2.22 thousand of years were found.

## 1. INTRODUCTION

Aeolian sediments have been studied with many purposes, they can be to understand sediment transportation, morphodynamic of dunefields, sea level variations and so on (Cunha, et al., 2017; Gianinni, et al., 2011; Keizars, et al. 2008). This work is interested in geochronology of aeolian sediments from Dama Branca (White Lady), Rio de Janeiro, Brazil, using the Trapped Charge Dating Techniques: Thermoluminescence (TL), Optically Stimulated Luminescence (OSL) and Electron Spin Resonance (ESR).

To date any sample (sediment, pottery, shell, bone, etc.) it's needed to define the start of the time counting. In the case of aeolian sediments, the sunlight is responsible to erase the signal and reset the clock (Wintle & Huntley, 1982).

For a sample exposed to the sun, there is a probability of eviction of a trapped electron, the rate of eviction is proportional to the intensity of the light, to the number of electrons and to the probability of eviction. For TL, this probability decreases over time, making it hard to completely reset the sample. As consequence, an unbleachable component is left, also known as "residual TL" (Aitken, 1985).

Huntley et al. (1985) proposed a new method of sediments dating based on OSL. Only electrons that can be released by absorption of visible light are used for  $D_e$  measurement, dispensing the need of residual signal calculations. With introduction of SAR protocol, Murray & Wintle (2003) proposed an improved OSL dating used nowadays for many researches to date aeolian sediments, fluvial sediments, pottery, etc. (Guangyin Hu, et al., 2017; Cano, et al., 2014).

Ikeya (1993) presented an extensive discussion of ESR applications in sediments dating. Toyoda, et al. (2000) evaluated the bleachability of several centers in quartz:  $E'1$ , Al, Ti-Li, Ti-H and Ti-Na. It was concluded that Ti-H and Ti-Na are the most sensitive centers to sunlight, being the best choice in aeolian sediment ESR dating, however, not all quartz samples exhibit Ti-Na signal and the Ti-H signal may be weak depending on the sample. Tsukamoto et al. (2015) emphasize the importance of samples pre-heating to remove the Ti-Li center thermally unstable component, reported by (Toyoda & Ikeya, 1994) interferes in the Dose Response Curve (DRC) and lead to mistakes in equivalent dose calculations.

Among these three techniques, OSL-SAR provides the best age estimation for aeolian sediments. TL can provide consistent as well, however, it will depend on the bleaching received for the sample while exposed to sunlight and previous dose that was experienced before sun exposure (Miallier, et al., 2006). ESR dating of sediments using Ti-Li center has potential to provide consistent results, bleaching tests have been done (Lu Gao, et al., 2009; Toyoda, et al., 2000; Tissoux, et al., 2007) and showed that the signal of Ti-Li center can be totally zeroed in nature and using sun simulators.

Here, it was dated 7 samples,  $D_e$  was measured by OSL-SAR to study the sand mobility and stabilization along migration direction. Two samples were dated by TL and ESR using the MAAD protocol for comparison, an alternative Multiple Aliquot Regenerative (MAR) protocol was evaluated for ESR. UV light exposition has been used for sample resetting instead high temperature annealing, the results between additive and regenerative protocol were compared.

## 2. MATERIALS AND METHOD

Dama Branca is a large dunefield found in Cabo Frio, Rio de Janeiro, Brazil (fig. 1). The formation of dunes in Cabo Frio and region can be summarized in three key aspects:

1) Cabo Frio has semi-arid weather conditions. According to Barbière (1975), from 1931 to 1970 the annual mean rainfall in Cabo Frio was below 100 mm from January up to November, only in December this value was higher than 100 mm.

2) Based on Castela & Barth (2006), it was identified that Cabo Frio is under persistent influence of upwelling, especially during the austral spring and summer. NE winds intensify the upwelling in the region, pushing the warmer water on the surface offshore and, as consequence, cold water emerges to surface.

3) Semi-arid conditions in Cabo Frio is strongly correlated with upwelling. It reduces rainfall since the cold water on the surface produces a negative balance between rainfall and water evaporation. The aerial view of Dama Branca dunefield (fig. 1) allow us to observe that the migration direction of sediments is influenced by winds from NE to SW, the same winds responsible to enhance upwelling in Cabo Frio.

The ages can be related, at a first approach, to episodes of arid and windy weather (Andrade, 2015).



**Figure 1 – Dama Branca dunefield seen from aerial photograph obtained from Google Earth Pro®. Migration of sediments is influenced by NE to SW winds.**

## 2.1. Sample Collection

Seven samples have been collected for dating using 100 cm long, 5 cm diameter and PVC pipes. Four samples were taken from DB position and three from 2DB position (fig. 2b and fig. 2c). At both positions, samples were collected at the base of a sand mound and from upper positions to evaluate the vertical age variation. At 2DB, a sample was collected from an inner position, using a 200 cm long and 5 cm diameter tube to study how ages vary into the mound (table 1). A trench of about 1m x 1m x 1m was open before inserting the tubes to avoid collecting samples from the surface.

Sediments from the ends of each tube were discarded. About 50 g of sediment to be used for OSL, TL and ESR measurements was weighted before and after thermal treatment at 50 °C for 24 h to calculate the water content.

Another portion of approximately 10 g was sieved to retain grains with 75  $\mu\text{m}$  and 180  $\mu\text{m}$ . The sieved portion underwent chemical treatment using HCl 10% followed by H<sub>2</sub>O<sub>2</sub> 27% to remove carbonates and organic materials, followed by HF 48% for 40 min to remove feldspars contamination and the  $\alpha$ -radiation contribution.

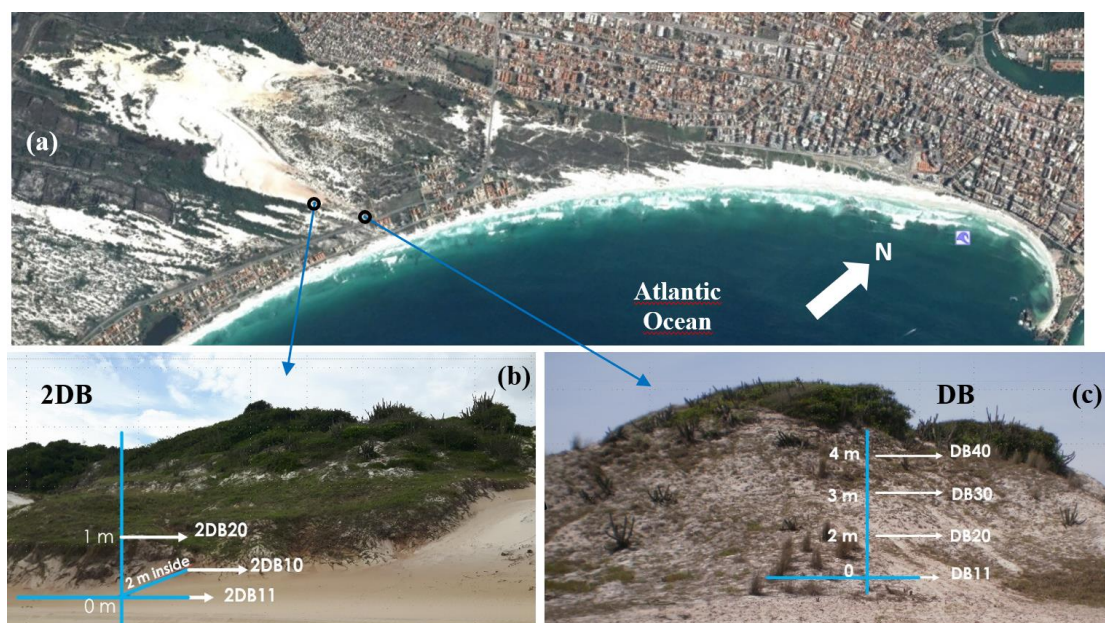


**Figure 2 – Sample collection points: a) aerial photograph of Dama Branca dunefield, b) 2DB position and c) DB position. Samples were collected from different point to study the age variation.**

**Table 1 – Geographic coordinates, height and depths of samples collection.**

Sample	Geographic coordinates	Relative height	Relative depth
DB11	22°54'35.1"S / 42°02'12.8"W	1 m	1 m
DB20	22°54'35.1"S / 42°02'12.8"W	2 m	1 m
DB30	22°54'35.1"S / 42°02'12.8"W	3 m	1 m
DB40	22°54'35.1"S / 42°02'12.8"W	4 m	1 m
2DB10	22°54'39.3"S / 42°02'19.8"W	Base (0 m)	2 m
2DB11	22°54'39.3"S / 42°02'19.8"W	Base (0 m)	1 m
2DB20	22°54'39.3"S / 42°02'19.8"W	1 m	1 m

## 2.2. Equivalent dose and annual dose rate measurement

OSL-SAR measurements were carried out using a Risø TL/OSL DA-20 in the East Carolina University (ECU) Luminescence Laboratory using the sequence showed in table 2. The reader has a 90Sr/90Y beta radiation source and blue LEDs (470 nm) and IR LEDs (870 nm) for stimulation. A Hoya filter (U-340 / 240-370 nm) separates the OSL signal from the stimulation blue light. De estimation was determined using Common Age Model and Central Age Model developed by Galbraith, et al. (1999), histograms and normal distributions were plotted to evaluate the De distribution.

**Table 2 - OSL-SAR sequence used in this work (Wintle & Murray, 2006)**

Step	Treatment	Observed
1	Dose $D_i$	--
2	Preheat	--
3	Stimulation for 100 s at 125 °C	$L_i$
4	Dose test $D_t$	--
5	Cut heat at 160 °C	--
6	Stimulation for 100 s at 125 °C	$T_i$
7	Return to 1	--

TL readouts were carried out using a model 4500 Harshaw TL reader in the Ionic Crystals, Thin Films and Dating Laboratory (LACIFID, in Portuguese) in the Physics Institute of University of São Paulo. The reader is equipped with two photomultiplier tubes that record the signal independently, the software WinREMS controls all reader functions. The MAAD protocol was used to estimate De and a method proposed by Cano, et al. (2013) was used to evaluate the residual TL. The heating rate used for recording TL signal was 4 °C/s. Each point in the glow curve represents a mean of five readouts (fig. 3a).

ESR measurements were performed using a X-band Freiberg MiniScope MS5000 spectrometer in the LACIFID equipped with a liquid nitrogen evaporation system that produces N<sub>2</sub> gas flow through the resonance cavity. Samples were cooled at -170 °C (203 K) to record the Ti-Li center. The experimental parameters were: microwave power 10 mW, modulation amplitude 0,15 mT, scan time 40 s, scan width 4 mT and the signal measurement is a result of

5 accumulated scans. The ESR intensity was measured based on Duval & Guilarte (2015) using  $g = 1.913$  peak-to-baseline signal. The interference with Ti-H center at  $g = 1.915$  can be neglected in most cases (fig. 3b). The ESR angular dependence was considered. Each aliquot was measured with three rotations and a scan is taken three times after every  $120^\circ$  azimuths rotation in the cavity, an average curve is taken to measure the quartz Ti-Li center intensity. The MAAD protocol was used to calculate  $D_e$ . It was also evaluated a multiple aliquot regenerative method using UV light exposure to reset the Ti-Li center, the result between additive and regenerative protocol have been compared and discussed. The amount of U,  $^{232}\text{Th}$  and  $\% ^{40}\text{K}$  was measured using a Canberra HPGe gamma spectrometer cooled with liquid nitrogen in LACIFID, it's equipped with a DSA-1000 and Genie 2000 v3.2 for spectrum acquisition and analysis. Each sample fills the  $236 \text{ cm}^3$  of the counting sealed support, the dried sample was weighted before measurement. The set was counted in the detector for 7 days, the spectrum is compared with standards soil samples (JR-1, JB3, JG-1a and JG-3) for determination of radionuclides concentrations. The concentration in ppm, geographic coordinates from where samples have been taken and the water content in each sample were uploaded to the Dose Rate and Age Calculator (DRAC) to calculate the annual dose rate ( $D_r$ ) (Durcan, et al., 2015).

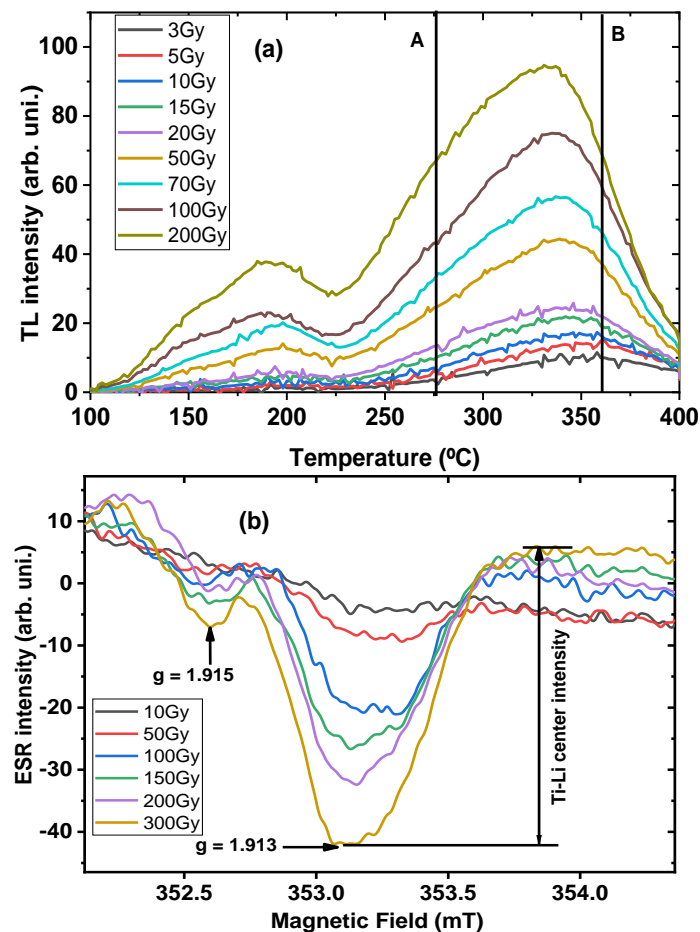


**Figure 3 – a) The sum of counts from 270 °C to 360 °C was taken as TL intensity and b) the peak-to-baseline height was taken as the ESR Ti-Li center intensity.**

### 3. RESULTS AND DISCUSSIONS

#### 3.1 OSL results

The SAR protocol was applied to measure  $D_e$  for each sample, plateau test was carried out to determine the preheat temperature. It was used 220 °C for 2DB10, 2DB11 and DB11, the left samples were preheated with 200 °C due to high recuperated signal exhibited when treated with 220 °C. The tests of recuperation, recycling and feldspar contamination were performed, the aliquot selection was based on Murray & Wintle (2003).

At least 24 aliquots per sample were read, a minimum of 16 aliquots are required for  $D_e$  calculation. The common age model (CoAM) and central age model (CAM) were applied based on the measured overdispersion for each sample based on Galbraith, et al. (1999). Fig. 4 shows the  $D_e$  distribution using histograms, normal distributions and as a probability function. Table 3 shows the ages measured for all studied samples.

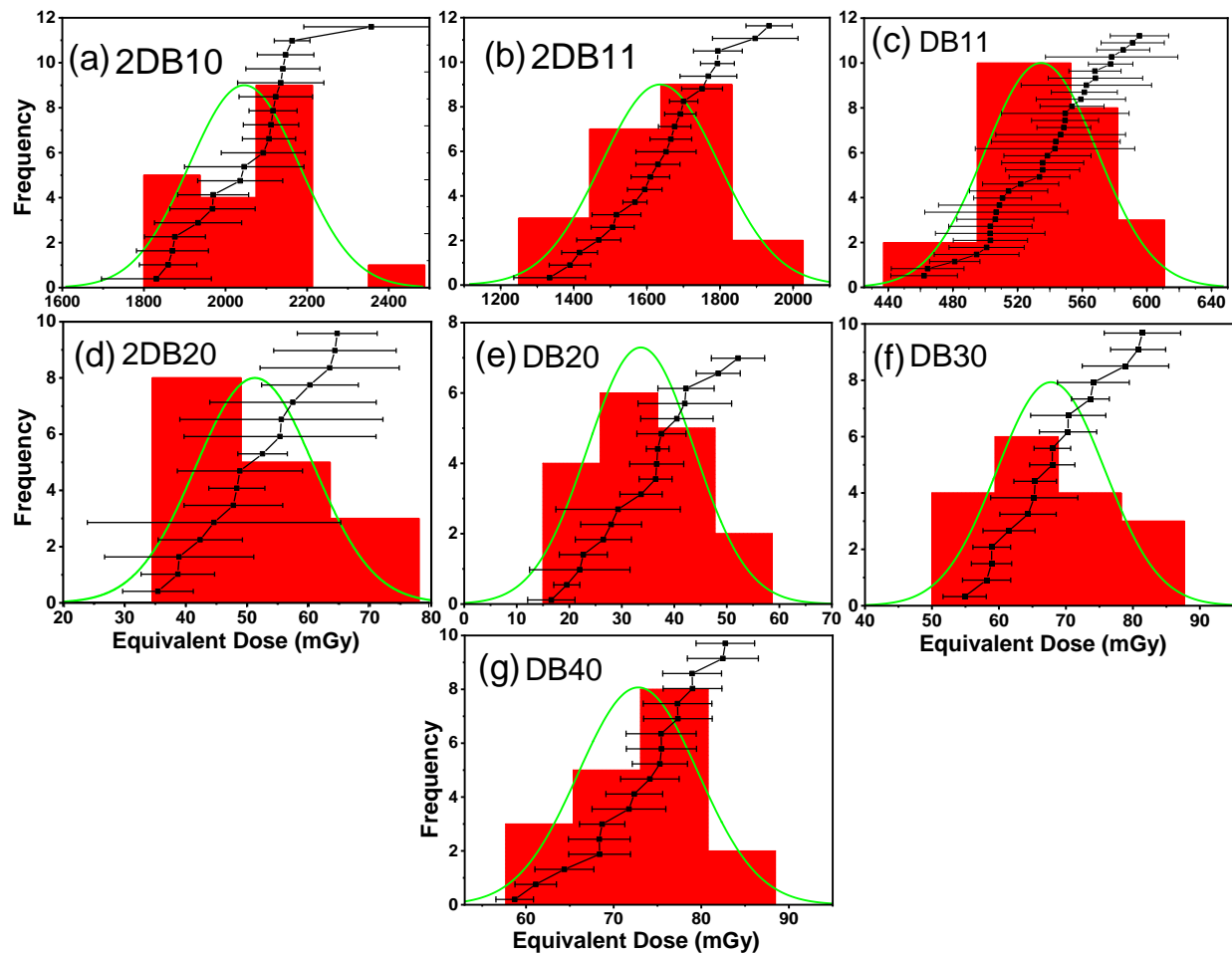


Figure 4 – Distribution of  $D_e$  measured for each sample.

**Table 3 – Concentration of radioisotopes, dose rate and samples age.**

Sample	U (ppm)	<sup>232</sup> Th (ppm)	<sup>40</sup> K (ppm)	D <sub>r</sub> with cosmic ray (mGy/year)	D <sub>e</sub> (mGy)	Overdispersion (%)	Age (kyears)
DB11	0.39 ± 0.02	0.69 ± 0.04	0.28 ± 0.01	0.69 ± 0.03	542 ± 17	5.38 ± 1.09	0.79 ± 0.04
DB20	0.26 ± 0.02	0.9 ± 0.04	0.27 ± 0.01	0.66 ± 0.03	34.8 ± 5.5	25.15 ± 6.04	0.05 ± 0.01
DB30	0.85 ± 0.05	4.26 ± 0.18	0.33 ± 0.01	1.051 ± 0.03	67.8 ± 2.3	9.84 ± 2.31	0.06 ± 0.01
DB40	1.47 ± 0.10	8.12 ± 0.40	0.36 ± 0.02	1.456 ± 0.05	67.1 ± 2.1	8.39 ± 1.90	0.05 ± 0.01
2DB10	0.91 ± 0.07	4.01 ± 0.22	0.18 ± 0.02	0.932 ± 0.04	2071 ± 67	7.90 ± 1.54	2.22 ± 0,12
2DB11	0.91 ± 0.05	4.62 ± 0.20	0.15 ± 0.01	0.958 ± 0.03	1647 ± 52	6.06 ± 2.08	1.72 ± 0.08
2DB20	0.47 ± 0.03	1.00 ± 0.04	0.29 ± 0.01	0.731 ± 0.03	52.1 ± 2.5	11.03 ± 5.59	0.07 ± 0.01

The samples DB11, 2DB10 and 2DB11 are sediments found in the base of DB and 2DB positions. They are the oldest samples; we can infer that sediments from these parts are more stable than sediments from upper parts. It was expected a gradual decrease in the age as the height from the base increases, but the ages showed that the sand mounds are rather formed by a stable base that is held by an active volume.

Fig. 5 shows the morphological changes of Dama Branca from 1984 to 2017, it was used images available on Google Earth Pro<sup>®</sup> taken at 1984, 2004 and 2017. Global Mapper<sup>®</sup> was used to calculate the sand covered areas and the migration rate.

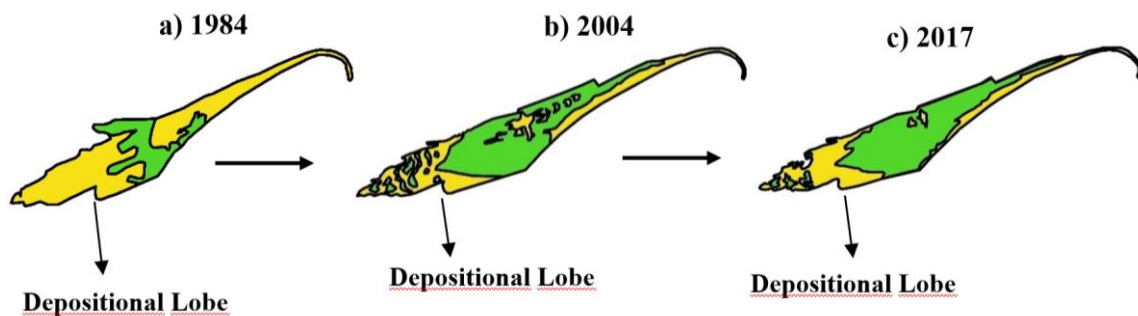


**Figure 5 – Morphological changes in Dama Branca. The depositional lobe records the sand movement from 1984 to 2017, an acceleration in the migration rate was detected in the last 13 years.**

The sand covered area (yellow) was drastically reduced, being 2.839 km<sup>2</sup> in 1984, 1.944 km<sup>2</sup> in 2004 and 1.215 km<sup>2</sup> in 2017. The migration rate is the maximum distance reached by the fastest depositional lobe divided by the elapsed time from the older to the newest aerial photograph (Mendes & Giannini, 2015). Between 1984 and 2004 (20 years) it was 2.54 m/year and between 2004 and 2017 (13 years) was 5.74 m/year.

This acceleration is related to the increase of wind power over aeolian supply (Mendes & Giannini, 2015). The increase in this ratio leads to an acceleration in the migration rate, as consequence the dunefield advances.



### 3.2 - TL Results

Multiple Aliquot Additive Dating protocol (MAAD) was used to calculate  $D_e$  by TL and ESR. Samples 2DB10 and 2DB11 were chosen for this study due to its natural ESR Ti-Li response. The left samples yielded very weak or even no natural signal response, being impossible to measure the Equivalent Dose.

TL measurements were done irradiating 9 aliquots of about 30 mg from 2 Gy up to 300 Gy, the sum of counts from 270 °C – 360 °C was taken as TL intensity. Each point in the dose response curve is a mean of 5 readouts, a single saturation exponential curve was used to fit the data (fig. 5a and 5b). It was found  $7.18 \pm 0.81$  Gy for 2DB10 and  $6.59 \pm 0.79$  Gy for 2DB11. The Residual TL correction was done using a 60 W fluorescent mercury lamp which has been calibrated with a Delta OHM HD 9021. The natural TL intensity ( $TL_0$ ) was measured, the residual TL ( $TL_R$ ) was taken after 300 min exposition under UV light, the following equation has been used to measure the corrected equivalent dose ( $D_{e,c}$ ).

$$D_{e,c} = D_e * \left(1 - \frac{TL_R}{TL_0}\right) \quad (1)$$

Fig. 6c and 6d shows the normalized integrated natural TL intensity in function of exposure time (min). In the first 100 min of exposition, for both samples the TL intensity reduces considerably for both samples, after that the bleaching rate decreases and as the time increases the intensity tends to a residual value. The size of  $TL_R$  is about 40% and 35% of the  $TL_0$  for 2DB10 and 2DB11, respectively (table 4).

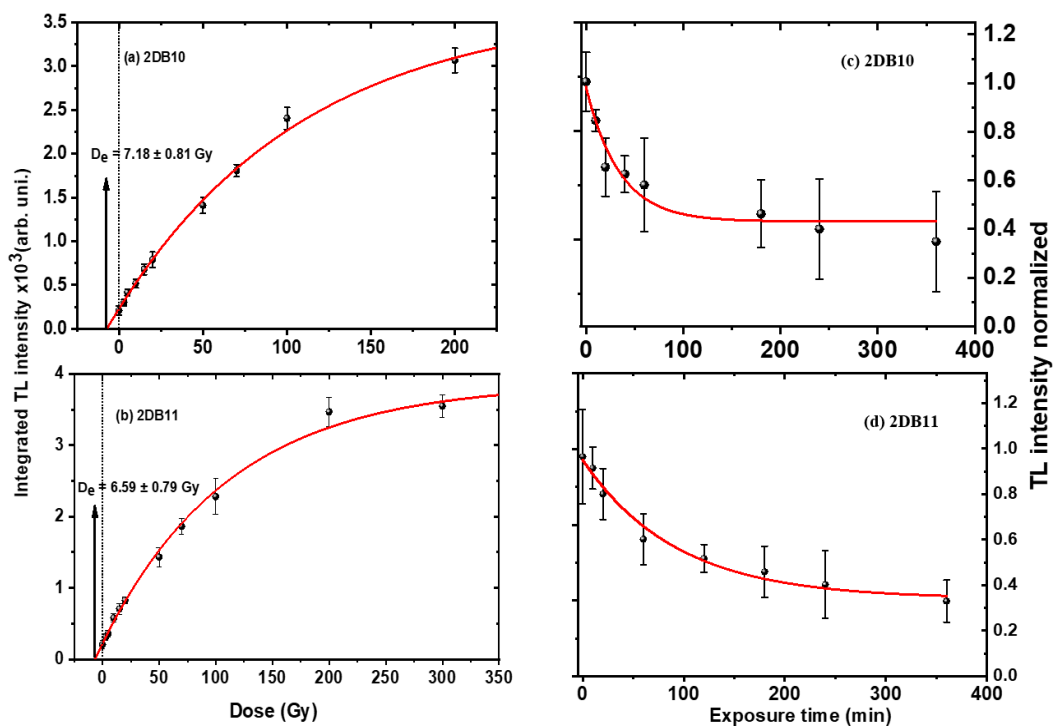


**Figure 6 – TL dose response curve for a) 2DB10 and b) 2DB11. The samples were bleached using UV light and the TL intensity as function of exposition time are presented in c) and d)**

**Table 4 – Ages measured by TL with residual TL correction**

Sample	TL <sub>R</sub> /TL <sub>0</sub>	1 - TL <sub>R</sub> /TL <sub>0</sub>	D <sub>e</sub>	D <sub>e,c</sub>	Age (kyears)
2DB10	0.40	0.60	7.18 ± 0.81	4.31 ± 0.49	4.62 ± 0.72
2DB11	0.35	0.65	6.59 ± 0.79	4.28 ± 0.51	4.46 ± 0.67

### 3.3 - ESR Results

ESR measurements were done with at least 5 aliquots of 100 mg, fig. 7 shows the pulsed annealing measurement for the natural ESR Ti-Li signal of 2DB10. The sample has been heated from 50 °C to 250 °C in 20 °C steps and held for 15 min at each temperature. The intensity is relatively stable from 80 °C to 150 °C. From this point, the intensity decreases and from 190 °C to 210 °C a second step appears, we assume that this second step is due to the thermally stable component of Ti-Li center and that this behavior is valid also to 2DB11, since they came from the same mound and location (Dama Branca). Based on this, the preheat temperature was defined to be 200 °C.

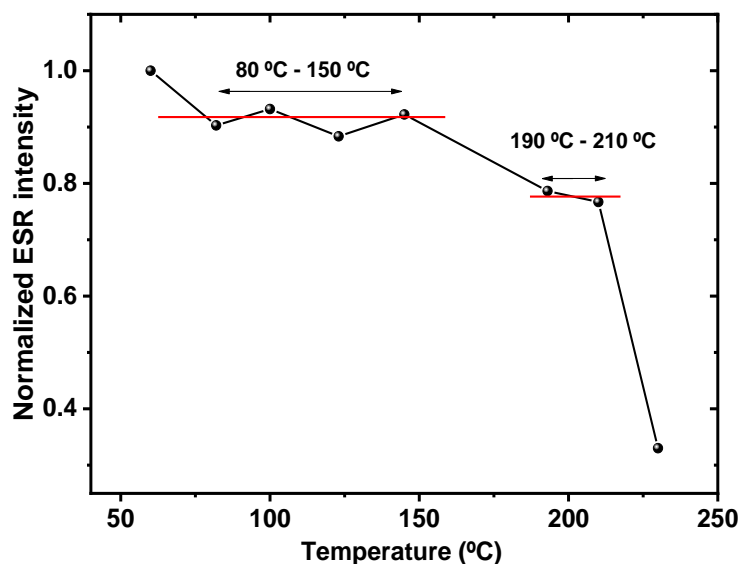


**Figure 7 – Pulsed annealing of 2DB10 sample. The thermally stable component of Ti-Li center is found at 190 °C – 210 °C.**

Fig. 8a and 8b show the dose response curve (DRC) for 2DB10 and 2DB11 without preheat, respectively, normalized by the mass measured after each readout. The samples showed a sublinear behavior with a rapidly growth from 150 Gy to 300 Gy.

Fig. 8c and 8d show the dose response curve after 200 °C preheat. The data was fitted using a single saturated exponential, it was found D<sub>e</sub> values of 15.65 ± 3.73 Gy (2DB10) and 13.32 ± 2.04 Gy (2DB11).

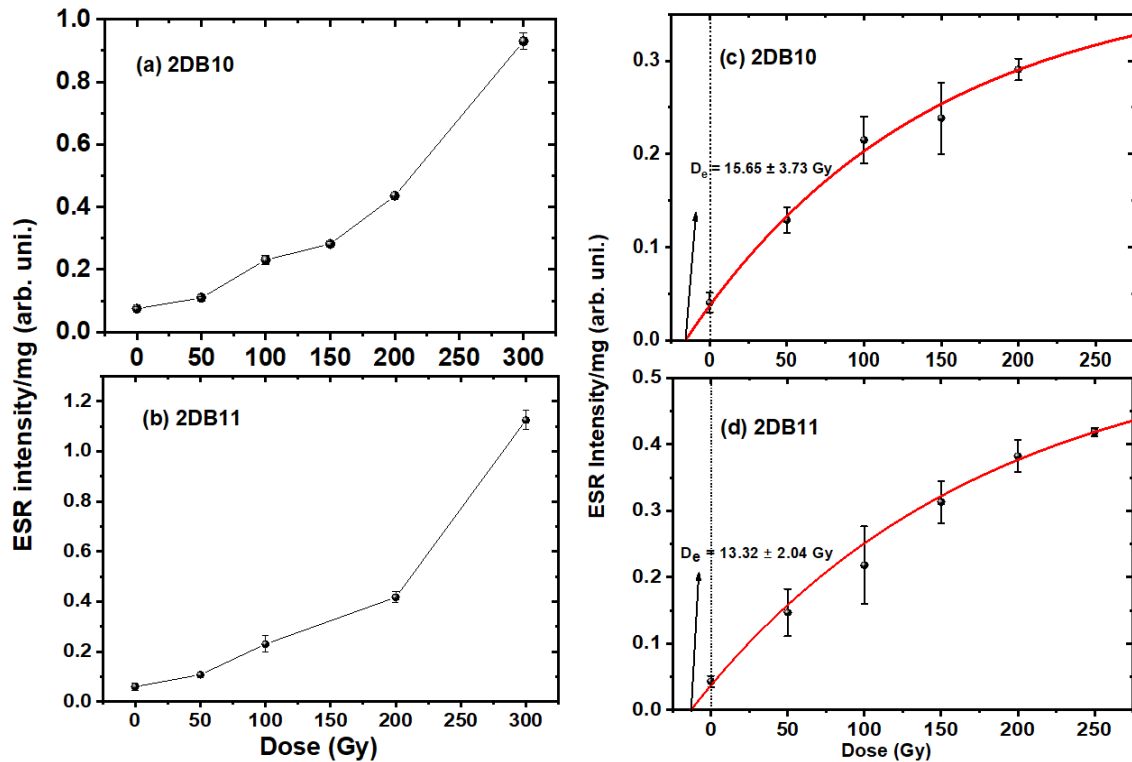


**Figure 8 – DRC of a) 2DB10 and b) 2DB11 without preheat. DRC c) and d) were obtained after 200 °C preheat.**

There are dramatic changes in the DRC curves for samples heated before measurements, our work doesn't provide enough information to explain why these changes occur, but the interference caused by the Ti-Li center thermally unstable component is discussed by Tsukamoto, et al., (2018).

Equivalent dose measured by ESR are overestimated if compared with TL and OSL, this can be due to incomplete bleaching in nature. Tissoux, et al., (2008) discuss that Ti-Li center, although being bleached faster than the Al center bleachable component showed overestimated  $D_e$  results compared to those obtained by Al. Studies about bleaching dynamics of Ti-Li center must be considered for dating aeolian sediments.

ESR dating using the regenerative method was evaluated, first, both samples were heated to 400 °C for 10 min to anneal Ti-Li center (Ikeya, 1993). Regenerative doses were given from 10 Gy to 250 Gy, samples were preheated at 200 °C before ESR measurements, fig. 9 shows the DRC for 2DB10.

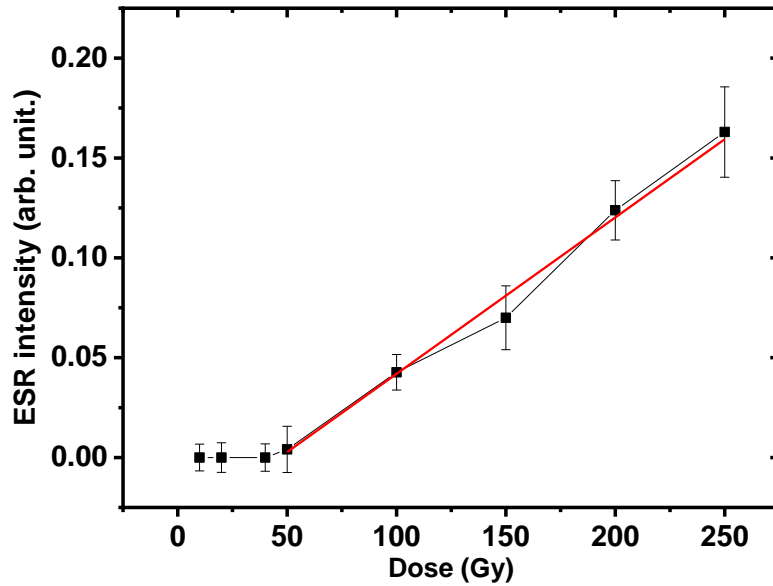


**Figure 9 – Regenerative dose response curve from 10 Gy to 250 Gy for Ti-Li center in 2DB10 sample. The ESR response in zero until a 50 Gy regenerative dose is given.**

Doses below 50 Gy did not induce ESR intensity in this sample. Within this dose range, the thermal annealing seems to change the sensitivity of Ti-Li center.

In a second attempt, 600 mg of sediments were spread on a plastic plate to form a uniform layer of quartz grains, the set was exposed to the 60 W fluorescent mercury lamp for 60 min. This time was enough to completely bleach the ESR Ti-Li center in our experiments. Regenerative doses were given from 10 Gy to 300 Gy, samples were preheated at 200 °C before ESR measurement, fig. 10 shows the DRC for both samples. The data was fitted using a single saturated exponential curve, the results are in good agreement with those obtained by the additive method (table 5).

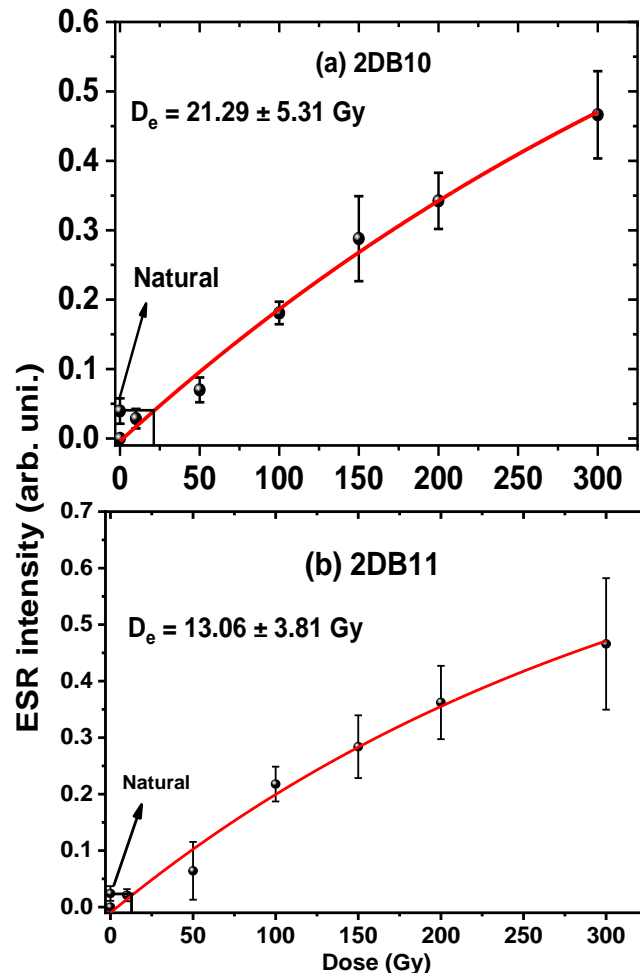


**Figure 10 – Regenerative dose response curves from 10 Gy to 300 Gy for Ti-Li center in a) 2DB10 and b) 2DB11 using UV light to reset the ESR signal. The data was fitted using a single saturated exponential curve.**

**Table 5 – Equivalent dose measured by additive DRC and regenerative DRC using UV light.**

Sample	ESR additive	ESR regenerative (UV light)
2DB10	$15.65 \pm 3.73$ Gy	$21.29 \pm 5.31$
2DB11	$13.32 \pm 2.04$ Gy	$13.06 \pm 3.81$

#### **4. CONCLUSIONS**

In this work sediments from a coastal dune filed known as Dama Branca were dated by OSL, TL and ESR using Ti-Li center. The OSL ages indicates that sediments from the base of the studied sand mounds are older at the base and younger at the top. This can be explained by the influence of NE to SW winds that are responsible for sand movement as seen in the morphological analysis. Equivalent dose measured by ESR Ti-Li center showed a great dependence upon preheat, which confirms the importance of this experimental procedure for ESR dating using the Ti-Li center. Unfortunately, the  $D_e$  values measured are higher compared with TL and OSL, this can indicate a poor bleaching of Ti-Li center in nature, leading to an overestimation of  $D_e$ . The regenerative DRC using UV light to reset the samples produced equivalent doses in agreement with those measured by additive DRC.

#### **ACKNOWLEDGMENTS**

To FAPESP (Fundação de Amparo à Pesquisa do Estado de São Paulo) for the grant n° 2015/21707-0 and n° 2014/03085-0. To IPEN for irradiating the samples and to the members of LACIFID that contributed to this work.

## REFERENCES

1. Aitken, M. J., 1985. *Thermoluminescence Dating*. London: Academic Press.
2. Andrade, H.A.A., 2015. *Evolução Sedimentar e Cronologia da Barreira Costeira Quaternária de Maçambaba: A Influência de Ventos de Rumos Opostos e seu Possível Significado Paleoclimático* (Dissertação de Mestrado), Universidade de São Paulo, São Paulo, 2015.
3. Barbière, E. B., 1975. *Ritmo climático e extração do sal em Cabo Frio*. Rev. Bras. Geografia **vol.37**, n.4, p. 23-109.
4. Cano, N.F., Munita, C. S., Watanabe, S., Barbosa, R. F., Chubaci, J.F.D., Tatumi, S. H., Neves, E. G., 2014. *OSL and EPR dating of pottery from the archaeological sites in Amazon Valley, Brazil*, Quaternary International, **Volume 352**, 176-180.
5. Castelão, R.M., Barth, J.A.C., 2006. *Upwelling conditions around Cabo Frio, Brazil: the importance of wind stress curl*. Geophysical Research Letters, **33**(L03062).
6. Cunha, A.M., Castro, J.W.A., Pereira, F.M.B., Carvalho, M.A., Suguio, K., 2017. *Variações do Nível Relativo do Mar Durante o Holoceno na Bacia do Rio Una, Cabo Frio - Rio De Janeiro: Aspectos Sedimentológicos, Faciológicos e Geocronológicos*, Revista Brasileira de Geomorfologia, Vol 18, 143-154.
7. Durcan, J.A., King, G.E., Duller, G.A.T., 2015. DRAC: Dose rate and age calculator for trapped charge dating. Quaternary Geochronology, 28, 54-61
8. Duval, M., Guilarte, V., 2015. ESR dosimetry of optically bleached quartz grains extracted from Plio-Quaternary sediment: Evaluating some key aspects of the ESR signals associated to the Ti-centers, Radiation Measurements 78, 28 – 41.
9. Galbraith, R. F., Roberts, R. G., Laslett, G. M., Yoshida, H., Olley, J. M., 1990. Optical dating of single and multiple grains of quartz from Jinmium Rock Shelter, Northern Australia: Part I, experimental design and statistical models, Archaeometry 41, 339 – 364.
10. Gao, L., Yin, G. M. Liu, C. R., Bahain, J.J., Lin, M., Li, J.P., 2009. Natural sunlight bleaching of the ESR titanium center in quartz, Radiation Measurements 44, 501-504.
11. Giannini, P.C.F., Sawakuchi, A.O., DeWitt, R., Nascimento Jr., D.R., Aguiar, V.A.P., Rossi, M.G., 2011. Determination of controls on Holocene barrier progradation through application of OSL dating: The Ilha Comprida Barrier example, Southeastern Brazil, Marine Geology, 285, 1-16.
12. Hu, G., Yu, L., Dong, Z., Jin, H., Luo, D., Wang, Y., Lai, Z., 2017. Holocene aeolian activity in the Headwater Region of the Yellow River, Northeast Tibet Plateau, China: A first approach by using OSL-dating, CATENA, Volume 149, Part 1, 150-157.
13. Huntley, D.J., Godfrey-Smith, D.I., Thewalt, M.L.W., 1985. Optical dating of sediments. Nature 313, 105–107.

14. Ikeya, M., 1993. *New Applications of Electron Spin Resonance: Dating, Dosimetry and Microscopy*, Singapore: World Scientific.
15. Keizars, K. Z., Forrest, B.M., Rink, W.J., 2008. Natural Residual Thermoluminescence as a Method of Analysis of Sand Transport along the Coast of the St. Joseph Peninsula, Florida, *Journal of Coastal Research*, Vol. 24, 500-507.
16. Mendes, V. R., Gianinni, P.C.F., 2015. Coastal dunefields of south Brazil as a record of climatic changes in the South American Monsoon System, *Geomorphology* 246, 22-34.
17. Miallier, D., Sanzelle, S., Pilleyre, T., Bassinet, C., 2006. Residual thermoluminescence for sun-bleached quartz: Dependence on pre-exposure radiation dose, *Quaternary Geochronology* 1, 313 – 319.
18. Murray, A.S., Wintle, A.G., 2003. The single aliquot regenerative dose protocol: potential to improvements in reliability. *Radiation Measurements* 37, 377–381
19. Tissoux, H., Falguères, C., Voinchet, P., Toyoda, S., Bahain, J.J., Despriée, J., 2007. Potential use of Ti-center in ESR dating of fluvial sediment, *Quaternary Geochronology* 2, 367-372.
20. Toyoda, S. Ikeya, M. 1994. ESR dating of quartz with stable component of impurity centers, *Quaternary Geochronology* 13, 625-628.
21. Toyoda, S., Voinchet, P., Falguères, C., Dolo, J. M., Laurent, M., 2000. Bleaching of ESR signals by the sunlight: a laboratory experiment for establishing the ESR dating of sediments, *Applied Radiation and Isotopes* 52, 1357–1362
22. Tsukamoto, S., Long, H., Richter, M., Li, Y., King, G.E., He, Z., Yang, L., Zhang, J., Lambert, R., 2018. Quartz natural and laboratory ESR dose response curves: A first attempt from Chinese loess, *Radiation Measurements*, in press (doi: 10.1016/j.radmeas.2018.09.008).
23. Tsukamoto, S., Toyoda, S. Tani, A., Oppermann, F., 2015. Single aliquot regenerative dose method for ESR dating using X-ray irradiation and preheat, *Radiation Measurements* 81, 9-15.
24. Wintle, A. G.; Huntley, D. J., 1982. Thermoluminescence dating of sediments *Quat. Sci. Rev.*, 1 (1982), pp. 31-51.